

Review

Interactions of protein antigens with antibodies

David R. Davies and Gerson H. Cohen

Laboratory of Molecular Biology, National Institute of Diabetes, Digestive and Kidney Diseases, National Institutes of Health, Bethesda, MD 20892-0560

ABSTRACT There are now several crystal structures of antibody Fab fragments complexed to their protein antigens. These include Fab complexes with lysozyme, two Fab complexes with influenza virus neuraminidase, and three Fab complexes with their anti-idiotype Fabs. The pattern of binding that emerges is similar to that found with other protein-protein interactions, with good shape complementarity between the interacting surfaces and reasonable juxtapositions of polar residues so as to permit hydrogen-bond formation. Water molecules have been observed in cavities within the interface and on the periphery, where they often form bridging hydrogen bonds between antibody and antigen. For the most part the antigen is bound in the middle of the antibody combining site with most of the six complementarity-determining residues involved in binding. For the most studied antigen, lysozyme, the epitopes for four antibodies occupy $\approx 45\%$ of the accessible surface area. Some conformational changes have been observed to accompany binding in both the antibody and the antigen, although most of the information on conformational change in the latter comes from studies of complexes with small antigens.

There has been a dramatic increase over the last 5 years in the number of Fab structures that have been determined by x-ray diffraction. It has been estimated that there are now >50 structures known to a resolution of between 3.0 and 2.0 Å, although the coordinates of many of these are not yet available in the Protein Data Bank (Chemistry Department, Brookhaven National Laboratory, Upton, NY). By contrast, the structures of Fab complexes with protein antigens, the subject of this review, have risen more slowly and have been restricted to a small group of antigens, notably hen egg white lysozyme (HEL) and influenza virus neuraminidase.

There have been a number of recent reviews of antibody structure and antibody-antigen associations (1–11). Braden and Poljak (11) in a recent review pay particular attention to the water molecules that surround the antibody-antigen interface and how these might influence the specificity. Whereas many of the general principles of these interactions, such as the

shape complementarity of the interacting surfaces, are now well established, the increasing data base, including the examination of complexes with mutant antibody or antigen, the calorimetric analyses of binding, and the application of new techniques to epitope mapping, add increasing detail to this picture. In this brief review, we shall describe the structures that are now available and discuss the results in terms of the mechanism of antibody-antigen recognition and binding.

Structures of Complexes with Protein Antigens

HEL. The most studied antigen has been HEL, and there are now five structures reported for complexes with this antigen. They are D1.3 (12–15), HyHEL-5 (16, 69), HyHEL-10 (17), D11.15 (18), and D44.1 (19).

The Fab (13) and Fv (14, 15) fragments of D1.3 have been studied as complexes with lysozyme. The structure of the isolated Fv has also been determined. The complex of the Fab of D1.3 with the Fab of an anti-idiotype to D1.3 has also been determined (20). The high resolution of the D1.3 Fv-HEL crystals permitted the identification of many water molecules, about 50 of which are located around the interface. Four water molecules are completely buried in the interface, with some located in the variable region light chain-heavy chain (V_L - V_H) interface. Titration calorimetry has been used to measure the thermodynamic parameters of the interaction (15). The reaction is enthalpically driven with some opposition from a negative entropy contribution, and it has been proposed that the bound waters play a major enthalpic role in the binding of antibody to antigen.

HyHEL-5 binds to a different epitope (Fig. 1) at the center of which are two arginine residues, Arg-45 and Arg-68, which are close to two glutamic acid residues on the Fab heavy chain, Glu-H35 and Glu-H50 (16, 69). The binding to lysozyme is quite strong, with an association constant of $4 \times 10^{10} \text{ M}^{-1}$ (23). The HyHEL-5-lysozyme complex contains several water molecules that are fully or partially buried in the interface. A cavity of about 250 \AA^3 is located between the V_H and V_L domains very close to the interface with lysozyme. This cavity contains three

water molecules between the V_L and V_H chains that contact only the Fab, together with a fourth water that makes hydrogen bonds to the bound lysozyme as well as V_H and V_L . The cavity in the HyHEL-5-lysozyme complex is located deeper in the V_H - V_L interface than that in the D1.3-lysozyme complex (15). Two other water molecules are located in a channel extending from bulk solvent into the lysozyme-Fab interface where they are involved in hydrogen bonding between the lysozyme and the Fab. An additional two waters are located on the interface periphery and serve as a bridge between two residues on the lysozyme and two on the Fab.

The association of HyHEL-5 with HEL has also been studied by titration calorimetry (24). The reaction is enthalpically driven with an unfavorable entropic contribution. The result is consistent with the loss of mobility upon association of the mobile complementarity-determining regions (CDRs), but it is concluded that the assignment of thermodynamic effects to particular intermolecular contacts is presently uncertain.

A lysozyme complex with Fab D44.1 has recently been reported at 2.5 Å (19). This antibody, for which the structure of the uncomplexed Fab has also been determined at 2.1 Å, binds to a lysozyme epitope that is remarkably similar to that of HyHEL-5. The interactions between the V_H residues Glu-H35 and -H50 and the Arg-45 and -68 of lysozyme are also qualitatively similar, although only two of the remaining hydrogen-bonding interactions are the same. The binding of the D44.1 to lysozyme, $1.4 \times 10^7 \text{ M}^{-1}$ (25), is significantly weaker than that of HyHEL-5, which might be explained by the existence of two hydrophobic holes within the interface.

HyHEL-5, D1.3, and a third monoclonal antibody (mAb), HyHEL-10 (17), form a group of epitopes that are essentially nonoverlapping. The epitopes for these and for another anti-lysozyme Fab, D11.15 (18), are shown in Fig. 1. For D11.15 the epitope partially overlaps that of D1.3. Together these four epitopes cover 45% of the molecular surface area

Abbreviations: HEL, hen egg white lysozyme; V_L and V_H , variable region light and heavy chains; CDR, complementarity-determining region; mAb, monoclonal antibody; HGH, human growth hormone.

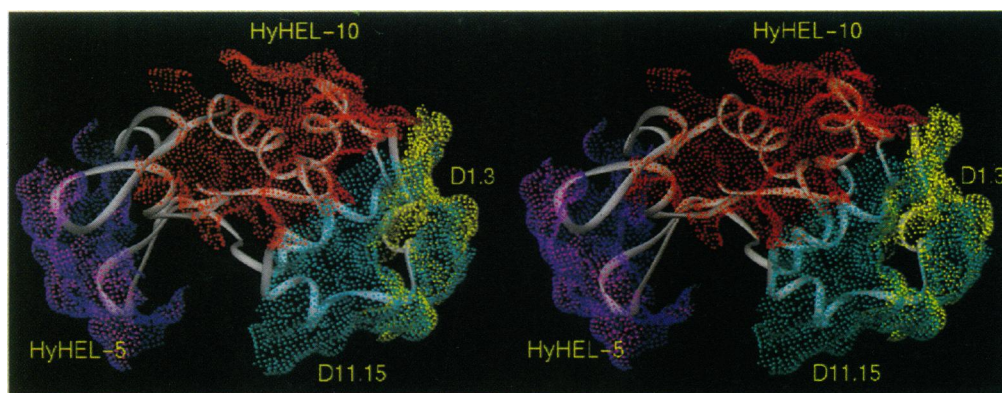


FIG. 1. RIBBONS diagram (21) of lysozyme surrounded by dot-surfaces representing the buried surface of the antigen when bound by the four antibodies HyHEL-5 (purple), HyHEL-10 (red), D1.3 (yellow), and D11.15 (blue). The buried surfaces were estimated with the program MS (22). Taken together, the four antibodies bury $\approx 45\%$ of the total molecular surface of the lysozyme molecule. Note the extensive overlap between the areas buried by D1.3 and D11.15, which amounts to $\approx 25\%$ of the individual areas buried by either of the two antibodies.

of the lysozyme. Examination of lysozyme epitopes by epitope mapping with a panel of 49 mAbs was able to account for $>80\%$ of the lysozyme surface (26). These data support the conclusion that the entire surface of HEL is potentially antigenic.

Influenza Virus Neuraminidase. Influenza virus neuraminidase is a tetramer of 60-kDa glycosylated polypeptide chains that is found attached to the membrane of the virus. A soluble form of the head can be released from the virus by protease digestion, and the crystal structure of this fragment of the N2 subtype neuraminidase has been determined (27, 28). The structure of the complex of the N9 neuraminidase and the Fab fragment of mAb NC41 has also been determined (29–31). The antibody is attached to the upper surface of the enzyme adjacent to the active-site pocket. The interface is extensive, with 1755 \AA^2 of combined surface area buried (Table 1). Five of the six

CDRs as well as light chain framework region 2 (FR2) make contact with the neuraminidase. As has been noted for other antibody–antigen complexes (1), the heavy chain makes more extensive contact with the antigen. They report no buried waters and emphasize the shape complementarity of the interacting surfaces. Two sugar residues from the carbohydrate attached to Asn-200 of an adjacent monomer are partly buried in the interface, contributing 38 \AA^2 to the interface.

The structure of a second antibody, NC10, has been crystallographically determined complexed to whale neuraminidase N9 (33, 34). The neuraminidase epitope for NC10 overlaps that for NC41, but although $\approx 80\%$ of each of the buried surface areas on the neuraminidase is contributed by residues common to both epitopes, these two antibodies bind quite differently to the neuraminidase. Only four of the CDRs of NC10 make contact

with the antigen; H1 and L2 do not. Although CDR H1 has the identical sequence in the two antibodies and appears to occupy the same location relative to the neuraminidase, the details of the structure reveal that in NC10, this CDR does not contact the antigen, whereas in CD41 it does. In the complex with NC10, carbohydrate attached to Asn-200 on an adjacent monomer is observed to form part of the epitope. One sugar residue from the oligosaccharide makes six contacts with NC10, and two other mannose residues have buried surface in the interface although they make no contact with the antibody. The buried carbohydrate surface area is 92 \AA^2 , making 13% of the total buried surface of the neuraminidase.

Histidine-Containing Phosphocarrier Protein. The structure of the complex of the protein HPr, the histidine-containing phosphocarrier protein of the phosphoenolpyruvate:sugar phosphotransfer-

Table 1. Antibody–antigen interface

Antibody*	Buried area [†] , \AA^2			H bonds, [‡] no.					Salt links, [‡] no.	Amino acids, ^{‡§} no.						Aromatic resids and contacting atoms, [¶] no.			
				Antibody		Antigen		Main- main		Contacting			Buried			Antibody		Antigen	
	V _L	V _H	Ag	Main	Side	Main	Side		V _L	V _H	Ag	V _L	V _H	Ag	Atoms	Resids	Atoms	Resids	
HyHEL-5	350	415	745	7	10	5	12	1	3	6	12	13	14	18	23	28	5	2	1
HyHEL-10	310	415	775	3	14	7	10	1	1	9	11	15	14	16	27	37	8	9	3
D1.3	275	330	635	3	12	7	8	1	0	8	9	16	13	12	24	35	9	2	1
D11.15	215	400	560	3	3	3	3	2	3	4	8	10	11	13	21	29	6	5	1
Jel42	200	420	650	4	4	1	7	1	0	5	14	13	8	17	21	19	8	3	1
NC41	420	480	855	3	9	5	7	0	0	10	10	20	15	21	32	28	8	9	1

*Antibody–antigen coordinates from HyHEL-5, Protein Data Base (PDB) code 3HFL; HyHEL-10, PDB code 3HFM; D1.3, PDB code 1VFB; D11.15, PDB code 1JHL; Jel42, PDB code 1JEL; and NC41, PDB code 1NCA.

[†]Buried surfaces were calculated by the program MS (22) with a probe of 1.7-\AA radius and are reported here for the V_L and V_H domains of the antibody and for the antigen (Ag).

[‡]Hydrogen bonds, salt links, and contacting atoms as calculated by the program CONTACTSYM (32). Contacting pairs of atoms are defined as those atom pairs that are located within the sum of the van der Waals radii of the two atoms plus 11% or are involved in hydrogen bonds or salt links (32). Main, main chain; side, side chain.

[§]The number of contacting and buried amino acids calculated with CONTACTSYM (32) and MS (22), as appropriate. They are reported separately for the V_L and V_H domains of the antibody and the antigen (Ag). The designation “buried” implies that the residue is at least partially inaccessible to bulk solvent because of the proximity of the interface surfaces of the antibody and the antigen. A probe of 1.7-\AA radius was used in the MS calculation.

[¶]Aromatic residues (resids) [His, Phe, Trp, Tyr] and atoms in contact as reported by CONTACTSYM (32) for the antibody and the antigen.

^{||}Calculations reported for the neuraminidase–NC41 complex consider protein–protein interactions only. Contributions to the surface due to the bound carbohydrate have been omitted.

ase system of *Escherichia coli*, and the mAb Jel42 has been determined (35). The interface has solvent-excluded surfaces of 650 Å² on HPr and 620 Å² on the antibody, consistent with the smaller size of the HPr (88 amino acid residues). One water molecule was observed buried in the interface. The antibody combining site is described as having a depression complementary to the HPr molecule rather like a baseball glove with the CDR L1 and CDR L3 forming the thumb and with the heavy chain CDRs in the depression. CDR L2 does not contact the HPr.

Antibody Anti-Idiotypic Complexes. The variability of the antibody CDRs results in new antigenic determinants that can in turn lead to the production of new antibodies, anti-idiotypic antibodies. The potential role of these antibody interactions in regulation of the immune system has been the subject of many investigations and much speculation (36, 37). The crystallographic determination of several idiotype-anti-idiotype complexes permits an examination of some of the structural aspects of these interactions. In addition to the possible regulatory role, there is also interest in the mechanisms by which anti-idiotypes can engage in mimicry through the formation of "internal images" (reviewed in ref. 38). Since both the antigen and the anti-idiotype antibody, Ab2, bind to the same antibody, Ab1, the potential for imaging exists, and functional imaging has been demonstrated for ligands that themselves interact with receptor molecules (reviewed in ref. 39). A possible example of internal imaging has been observed by Garcia *et al.* (39), who examined an anti-anti-idiotype Fab, Ab3, that binds strongly to the antigen, angiotensin II. In the complex with Ab3, the angiotensin II, an octapeptide, adopts a conformation that resembles the CDR3 of a light chain, suggesting a possible mechanism for the interactions in which a CDR of Ab2, presumably CDR3 of the light chain, would carry a similar conformation.

Three structures have been reported for complexes between antibody Fabs and their anti-idiotype Fabs. The first involves the anti-lysozyme antibody D1.3, permitting a comparison of the antibody (Ab1) complexed with the antigen and with Ab2 (20). The complex interface is similar to those observed in other antibody-protein interactions. The anti-idiotype antibody binds to 13 amino acids on D1.3, mainly from the CDRs; 7 of these amino acids make contacts with lysozyme. The two surfaces demonstrate considerable shape complementarity with about 800 Å² of each surface buried in the interface. The main chain conformation of the D1.3 CDRs in the complex shows no important differences from the complex with lysozyme, although the side chains of three CDR residues differ considerably. The authors were unable to find structural

evidence for an internal image. The residues common to the anti-idiotype and to lysozyme carry out different functions for the most part in the two complexes. They observe that the epitope on lysozyme contains an α -helix, which is unlikely to be found in the CDRs of antibodies, so that for this example mimicry is unlikely to be observed.

The association of D1.3 with two anti-idiotypic antibodies, E225 and E5.2, has been studied by titration calorimetry (40). For E5.2 the results are similar to those observed for HyHEL-5 and D1.3 with HEL and for many other protein-protein interactions (41)—namely, a negative enthalpy change accompanied by a negative entropy change. However, for E225, which binds weakly to D1.33 ($K_a = 2 \times 10^5 \text{ M}^{-1}$), the reaction is entropy-driven with only a small positive enthalpy change.

A more recent study has been reported of an anti-idiotype Fab complexed with the Fab of an antibody against the E2 peplomer, a glycoprotein from feline peritonitis virus (42). Again the shape complementarity between the two interacting surfaces is good, and no waters are observed in the interface although the resolution is low (2.9 Å) for reliable water observation. In this complex the heavy chains of the antibodies dominate the interactions, accounting in both cases for about three-quarters of the interacting surfaces. The structure of the antigen is not known, but the antibody binds to antigen on Western blots, where it is probably denatured. Each of the CDRs L1 and H1 of Ab2, which both interact extensively with Ab1, contain six amino acids that virtually mimic sequences within the antigen. When Ab2 is injected into mice, it elicits the production of Ab3s that have feline infectious peritonitis virus-neutralizing properties. It is tempting to speculate again that this similarity between the CDRs of Ab2 and corresponding regions of the antigen might provide an explanation for internal imaging. However, experimental support for this model will require the determination of the antigen structure complexed to Ab1.

A third complex of an antibody Fab with anti-idiotype Fab has been reported (43) in which the antibody is specific for a cell wall homopolysaccharide. The authors conclude that the putative polysaccharide-binding cleft on the Ab1 is too narrow and deep to allow comprehensive contact with Ab2, thus accounting for the inability of the Ab2 to carry an internal image of the antigen.

Amino Acid Composition of Antibody Combining Sites

The question of whether antibody combining sites have unusual amino acid compositions has been addressed by several groups. Kabat *et al.* (44) analyzed the

relative frequency of different amino acids in the CDRs and observed that asparagine and histidine residues were about twice as likely to appear in the CDRs as in the framework. Padlan (45) calculated an amino acid propensity for the CDRs (based on the frequency with which the amino acid was observed in the CDRs versus its frequency in the framework residues of the variable domains) and noted that asparagine and histidine were 8 times more likely to appear in the CDRs than in the framework and that tyrosine residues were 3 times more likely to be present. Padlan also enumerated the antigen-contacting residues in the paratope and observed a high proportion of tyrosine and tryptophan. Janin and Chothia (46) compared the interacting surfaces of four antibody-protein complexes with a group of protease-inhibitor complexes. They observed very similar properties for the two sets of interacting surfaces, the major difference being the high density of aromatic residues in the antibody-combining sites. Mian *et al.* (47) examined the antigen-binding residues in six crystallographically determined antibody-antigen complexes and concluded that tryptophan, tyrosine, serine, and asparagine residues were most abundant.

Recently, Lea and Stuart (48) measured the percentage contribution of the different amino acid species to the total accessible surface of the CDRs and compared this with the corresponding values for a control group of proteins and for four picornaviruses. They found that the serine residues within the immunoglobulin CDRs have a significantly higher fractional surface area contribution than the control group. Using this criterion, they also concluded that the above-average contribution of tyrosine to the CDRs is barely statistically significant and that histidine and asparagine have average contributions. Padlan (45) did not observe a high propensity for serine, and the differences between his data and those of Lea and Stuart can probably be accounted for by the different criteria used to define the relative amino acid contributions, such as the greater abundance of serine in the framework residues that Padlan used as a control.

Table 1 shows a summary of the physical properties of the interfaces for the six complexes for which coordinates are available in the Protein Data Bank. It is clear that a high percentage (34%) of the antibody-contacting residues are aromatic in character; of these more than two-thirds are tyrosine residues. In contrast, the contacting residues on the antigens contain relatively few that are aromatic. Fig. 2 shows the contacting aromatic residues observed in the HyHEL-10-lysozyme complex (7, 17). These include Tyr-H33, which penetrates the substrate binding groove of lysozyme.

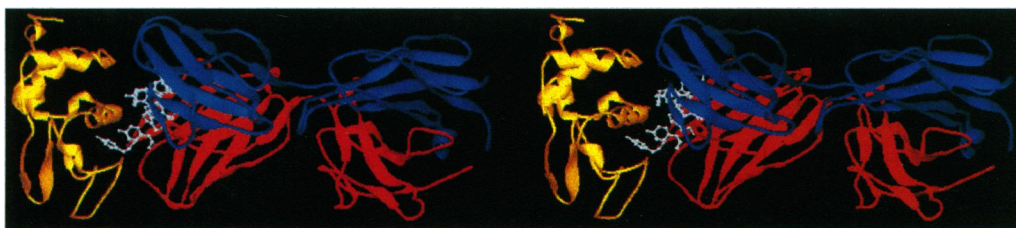


FIG. 2. RIBBONS diagram (21) of the HyHEL-10-lysozyme complex showing the aromatic residues in the combining site that contact the antigen. This figure prepared by Susan Chacko.

Padlan (7, 45) also calculated from the x-ray data the fractional solvent exposures of the individual amino acid species in the CDRs of seven antibodies and compared these with their corresponding exposures when in the framework region of the Fv fragments. He observed that the aromatic residues tyrosine and tryptophan in the CDRs were significantly more solvent-exposed.

Epitope Mapping

Crystallographic investigations of antibody-antigen complexes provide an opportunity to compare predictions from epitope mapping with direct observation of the contacting residues. There have been extensive studies of epitopes by the use of peptides in which an antibody produced in response to a protein antigen can be examined for binding to peptides from that antigen. For HEL, these methods have recently been reviewed (49). The epitope for lysozyme with HyHEL-5 was successfully predicted (50) based on the availability of a library of avian lysozymes that were presumed to have approximately the same tertiary structure, but with small differences in the amino acid sequences. This method is of course limited by the diversity of the available library. The application of mutagenesis techniques has now become a powerful method for epitope mapping (51, 52).

There has been an interesting application of site-directed mutagenesis to distinguish between two structures that had been proposed for the protein HPr (53). The three-dimensional structure had been determined by two-dimensional NMR and by x-ray diffraction (54, 55), and there were major differences between the two structures. The effect of mutations on the binding of two antibodies, Jel42 and Jel44, revealed that when the putative epitope was mapped on each of the proposed structures, the epitope for Jel44 was only consistent with the two-dimensional NMR structure of HPr for which it gave a contiguous binding surface. In contrast, the model derived from x-ray diffraction produced a scattered distribution of these residues in which some were buried and others were surrounded by noninvolved residues. Subsequently the epitope predicted in these experiments for Jel42 was confirmed by an x-ray diffraction analysis

of the complex of the Fab with HPr, in which the structure observed for HPr was that determined by the NMR analysis (35). Of the 14 amino acid residues that interact with the Jel42 binding site, 9 were correctly identified.

The epitope on cytochrome *c* for a monoclonal antibody has been defined by hydrogen exchange in two-dimensional NMR (56). This method can be used for a protein antigen when the protein is small enough for the ^1H NMR resonances to be determined. Eleven residues in three different segments of sequence were identified that formed a structurally related patch on the surface with a water-accessible surface area of about 750 \AA^2 . There has been a preliminary report of the crystallization of an antibody Fab to cytochrome *c*, both free and complexed with the antigen (57).

Conformational Changes that Accompany Complex Formation

The interaction of antibody with antigen involves conformational changes in both the antibody and the antigen that can range from insignificant to considerable. In general, the formation of a complex will adopt many of the characteristics of induced fit, similar to those seen in other macromolecular interactions. The changes that may occur in the antibody upon binding consist of combinations of simple side-chain movements, concerted movements of individual CDRs, and displacement of V_H relative to V_L . Most of the information on conformational changes upon antigen binding has come from nonprotein antigens, where the antibody has also been crystallized in the absence of antigen. Each of the kinds of movement described above has been observed for these complexes and these have been reviewed (10, 58, 59). Some of the conformational changes observed are quite large, with the largest V_H - V_L rearrangement occurring in an Fab complex with a human immunodeficiency virus peptide (59). Changes of this nature will considerably complicate attempts to model antibody combining sites.

For protein antigens, the antibody D1.3 has been examined as an unbound Fv fragment, as an Fab and an Fv complexed to lysozyme, and as Fab complexed to E225, an anti-idiotope. The differences

between the bound and unbound Fv structures are minimal and include small adjustments of the side chains together with a small movement of V_H relative to V_L (14). The interaction of the variable domains has been reviewed (5), and it was noted that the contacting surface between V_H and V_L contained $\approx 40\%$ contribution from the CDRs. This can result in significant differences in the angle of rotation between V_H and V_L , which varies from 165° to 180° . Changes in this angle were originally hypothesized for the NC41-neuraminidase complex (29), and substantial changes have now been observed in several instances when Fabs are complexed to small ligands (10, 59). The differences between unbound and bound D1.3 in its complex with E225 (20) include several significant side-chain movements of the D1.3 antibody relative to the uncomplexed structure (40).

We have analyzed four of the crystal complexes with lysozyme that clearly demonstrate that the interaction of antibody with antigen can produce significant conformational changes in the antigen, mainly in regions that are demonstrably flexible. Lysozyme alone can be crystallized in a number of crystal forms. A comparison of the tetragonal (60), monoclinic (61), and triclinic (62) forms, which provide four independent structures, demonstrates the flexibility of the surface loops. When the two independent molecules in the monoclinic form are superimposed, they have a rms deviation of 0.64 \AA for the C^α atoms, but the C^α atoms of Gly-71 and Gly-102 are displaced by 3.68 \AA and 3.40 \AA , respectively, from the corresponding position in the other molecule. In a similar comparison of the triclinic and tetragonal molecules, with overall rms = 0.65 \AA , the relative displacements of the C^α atoms of Thr-47 and Asn-103 are 2.73 \AA and 2.64 \AA , respectively. Residue Thr-47 in the tetragonal crystal makes a packing contact with a neighboring molecule that might explain the observed conformational difference for that residue.

In a similar manner we have compared the conformations of the lysozyme molecules bound to HyHEL-5 (69), HyHEL-10 (17), D1.3 (15), and D11.15 (18). The rms match against the mean set of coordinates for the ensemble was 0.54 \AA . The largest C^α separation for the superimposed lysozymes was 8.17 \AA between the Gly-102

residues of D1.3 and D11.15. There were also differences of 2.48 Å between the Pro-70 and 2.16 Å between the Thr-47 C α atoms of HyHEL-5 and HyHEL-10. These are substantial changes that confirm the flexibility in these regions of lysozyme noted in the uncomplexed molecules. The HyHEL-5 epitope includes both Thr-47 and Pro-70. Gly-102 is part of the buried interface in HyHEL-10, D1.3, and D11.15. In D1.3 the residues Gly-102 and Asn-103 are displaced by 8 Å from their positions in HyHEL-10 and D11.15 so as to participate in the interface surface. The flexibility therefore permits the enhancement of the complementarity at these three points on the antigen surface.

Mutational Effects on Antibody-Antigen Binding

Mutations in either antibody or antigen can be used to analyze the contributions of individual residues to the formation of the complex. There have been several such studies where the binding effects have been correlated with the known three-dimensional structure.

The power of mutational analysis has been demonstrated in a comparison of the structural and functional epitopes for the human growth hormone (HGH)-receptor system by a mutational analysis of the interacting residues on the HGH in which each residue in turn was replaced by alanine (51, 52). It was found that only one-quarter of the buried side chains could account for most of the binding energy. The predominant role of these side chains is to slow the dissociation of the complex. A similar analysis of the receptor epitope (52, 63) revealed a complementary hot spot on the receptor surface where there is a hydrophobic region dominated by two tryptophan residues, which accounts for more than three-quarters of the binding energy.

Chacko *et al.* (64) have examined the changes in the HyHEL-5-lysozyme complex that accompany the "conservative" substitution of lysine for arginine at position 68 of lysozyme. The mutation produces a decrease by a factor of 1000 in the binding from 10^{11} to 10^8 M $^{-1}$, as was observed in the binding to bob-white quail, which has this mutation in the epitope region (65). Comparison of the crystal structures of the complex shows that essentially no changes take place in the interior of the interface except in the immediate vicinity of the mutation site, and there is little change in the buried surface area. A water molecule replaces the two nitrogens of the guanidinium group of the arginine and partly compensates for the loss of the two salt bridges between the Arg-68 and Glu-H50. The net result of the substitution is a loss of hydrogen bonding in that the side-chain amino group of the lysine is unable to

make the same bonding arrangement as the guanidinium group of the arginine.

Tulip *et al.* (66) examined two complexes of mutant neuraminidase with NC41. The mutations Asn-329 \rightarrow Asp and Ile-368 \rightarrow Arg produced only a slight reduction in affinity. Both structures demonstrate that local structural rearrangements can be used to accommodate these amino acid substitutions.

Chitarra *et al.* (18) have determined the structure of a complex of pheasant lysozyme (PHL) with the Fv of D11.15, an antibody generated against chicken lysozyme that binds about 4 or 5 times better to pheasant and guinea fowl lysozyme. The Fv contacts involve all three heavy chain CDRs but only the third CDR of the light chain. There are two amino acid differences that might cause the observed difference in binding. The first is Asn(HEL)-113 \rightarrow Lys(PHL) where the lysine makes nonpolar contacts with Tyr-H57. However, modeling the asparagine in this position indicates that it too could make nonpolar contacts with the antibody. The second difference is Gln(HEL)-121 \rightarrow Asn(PHL), where the Asn-121 is 3.9 Å away from light chain Ser-L30. Modeling with a glutamine in this position shows that it could make a hydrogen bond with Ser-L30. These results illustrate the difficulty of providing a structural explanation for complexes where the differences in binding energies are so small.

The effect on the D1.3 lysozyme complex of a substitution of leucine for tryptophan in position 92 of the light chain has been reported (67). This change results in a decrease in affinity by a factor of about 1000. They measure a change in the ΔH of association of 3.8 kcal and state that the entropy is not affected. The structure shows that in the mutant complex, the space occupied by the tryptophan is taken up by two water molecules and the buried area in the complex decreases by about 150 Å 2 .

Conclusion

In view of the enormous diversity of the immune response, it is perhaps presumptuous to expect that the few examples discussed above can totally describe antibody-antigen interactions. However, from these results it is apparent that these associations have much in common with other protein-protein interactions (2, 68). The results from thermodynamic, structural, and mutational analyses demonstrate many similarities with those observed for other protein systems. The only significant difference seems to be in the clustering of aromatic residues in the antibody combining site, and it is interesting that the recent mutational study of the HGH receptor (52) identifies a hot spot of binding at the two tryptophans in the middle of the receptor interface.

We are grateful to Drs. Edward Padlein and Susan Chacko for helpful discussions.

- Davies, D. R., Padlan, E. A. & Sheriff, S. (1990) *Annu. Rev. Biochem.* **59**, 439-473.
- Janin, J. & Chothia, C. (1990) *J. Biol. Chem.* **265**, 16027-16030.
- Colman P. M. (1991) *Curr. Opin. Struct. Biol.* **1**, 232-236.
- Davies, D. R. & Chacko, S. (1993) *Acc. Chem. Res.* **26**, 421-427.
- Sheriff, S. (1993) *ImmunoMethods* **3**, 222-227.
- Wilson, I. A. & Stanfield, R. L. (1993) *Curr. Opin. Struct. Biol.* **3**, 113-118.
- Padlan, E. A. (1994) *Mol. Immunol.* **31**, 169-217.
- Webster, D. M., Henry, A. H. & Rees, A. R. (1994) *Curr. Opin. Struct. Biol.* **4**, 123-129.
- Padlan, E. A. (1994) *Antibody-Antigen Complexes* (Landes, Austin, TX).
- Wilson, I. A. & Stanfield, R. L. (1994) *Curr. Opin. Struct. Biol.* **4**, 857-867.
- Braden, B. C. & Poljak, R. J. (1995) *FASEB J.* **9**, 9-16.
- Amit, A. G., Mariuzza, R. A., Phillips, S. E. V. & Poljak, R. J. (1986) *Science* **233**, 747-753.
- Fischmann, T. O., Bentley, G. A., Bhat, T. N., Boulot, G., Mariuzza, R. A., Phillips, S. E. V., Tello, D. & Poljak, R. J. (1991) *J. Biol. Chem.* **266**, 12915-12920.
- Bhat, T. N., Bentley, G. A., Fischmann, T. O., Boulot, G. & Poljak, R. J. (1990) *Nature (London)* **347**, 483-485.
- Bhat, T. N., Bentley, G. A., Boulot, G., Greene, M. I., Tello, D., Dall'Acqua, W., Souchon, H., Schwartz, F. P., Mariuzza, R. A. & Poljak, R. J. (1994) *Proc. Natl. Acad. Sci. USA* **91**, 1089-1093.
- Sheriff, S., Silverton, E. W., Padlan, E. A., Cohen, G. H., Smith-Gill, S. J., Finzel, B. C. & Davies, D. R. (1987) *Proc. Natl. Acad. Sci. USA* **84**, 8075-8079.
- Padlan, E. A., Silverton, E. W., Sheriff, S., Cohen, G. H., Smith-Gill, S. J. & Davies, D. R. (1989) *Proc. Natl. Acad. Sci. USA* **86**, 5938-5942.
- Chitarra, V., Alzari, P. M., Bentley, G. A., Bhat, T. N., Eiselé, J.-L., Houdusse, A., Lescar, J., Souchon, H. & Poljak, R. J. (1993) *Proc. Natl. Acad. Sci. USA* **90**, 7711-7715.
- Braden, B. C., Souchon, H., Eiselé, J.-L., Bentley, G. A., Bhat, T. N., Navaza, J. & Poljak, R. J. (1994) *J. Mol. Biol.* **243**, 767-781.
- Bentley, G. A., Boulot, G., Riottot, M. M. & Poljak, R. J. (1990) *Nature (London)* **348**, 254-257.
- Carson, M. (1991) *J. Appl. Crystallogr.* **24**, 958-961.
- Connolly, M. L. (1983) *J. Appl. Crystallogr.* **16**, 548-558.
- Benjamin, D. C., Williams, D. C., Jr., Smith-Gill, S. J. & Rule, G. S. (1992) *Biochemistry* **31**, 9539-9545.
- Hibbitts, K. A., Gill, D. S. & Willson, R. C. (1994) *Biochemistry* **33**, 3584-3590.
- Tello, D., Goldbaum, F. A., Mariuzza, R. A., Ysern, X., Schwarz, F. P. & Poljak, R. J. (1993) *Biochem. Soc. Trans.* **21**, 943-946.
- Newman, M. A., Mainhart, C. R., Mallett, C. P., Lavoie, T. B. & Smith-Gill, S. J. (1992) *J. Immunol.* **149**, 3260-3272.

27. Varghese, J. N., Laver, W. G. & Colman, P. M. (1983) *Nature (London)* **303**, 35–40.
28. Varghese, J. N. & Colman, P. M. (1991) *J. Mol. Biol.* **221**, 473–486.
29. Colman, P. M., Laver, W. G., Varghese, J. N., Baker, A. T., Tulloch, P. A., Air, G. M. & Webster, R. G. (1987) *Nature (London)* **326**, 358–363.
30. Tulip, W. R., Varghese, J. N., Webster, R. G., Air, G. M., Laver, W. G. & Colman, P. M. (1989) *Cold Spring Harbor Symp. Quant. Biol.* **54**, 257–263.
31. Tulip, W. R., Varghese, J. N., Laver, W. G., Webster, R. G. & Colman, P. M. (1992) *J. Mol. Biol.* **227**, 122–148.
32. Sheriff, S., Hendrickson, W. A. & Smith, J. L. (1987) *J. Mol. Biol.* **197**, 273–296.
33. Malby, R. L., Tulip, W. R., Harley, V. R., McKim-Breschkin, J. L., Laver, W. G., Webster, R. G. & Colman, P. M. (1994) *Structure* **2**, 733–746.
34. Colman, P. M. (1994) *Protein Sci.* **3**, 1687–1696.
35. Prasad, L., Sharma, S., Vandonselaar, M., Quail, J. W., Lee, J. S., Waygood, E. B., Wilson, K. S., Dauter, Z. & Delbaere, L. T. J. (1993) *J. Biol. Chem.* **268**, 10705–10708.
36. Jerne, N. K. (1974) *Ann. Immunol. C* **125**, 373–389.
37. Gaulton, G. N. & Greene, M. I. (1986) *Annu. Rev. Immunol.* **4**, 253–280.
38. Pan, Y., Yuhasz, S. C. & Amzel, L. M. (1995) *FASEB J.* **9**, 43–49.
39. Garcia, K. C., Ronco, P. M., Verroust, P. J., Brünger, A. T. & Amzel, L. M. (1992) *Science* **257**, 502–507.
40. Tello, D., Einstein, E., Schwarz, F. P., Goldbaum, F. A., Fields, B. A., Mariuzza, R. A. & Poljak, R. J. (1994) *J. Mol. Recognit.* **7**, 57–62.
41. Ross, P. D. & Subramanian, S. (1981) *Biochemistry* **20**, 3096–3102.
42. Ban, N., Escobar, C., Garcia, R., Hasel, K., Day, J., Greenwood, A., McPherson, A. (1994) *Proc. Natl. Acad. Sci. USA* **91**, 1604–1608.
43. Evans, S. V., Rose, D. R., To, R., Young, N. M. & Bundle, D. R. (1994) *J. Mol. Biol.* **241**, 691–705.
44. Kabat, E. A., Wu, T. T. & Bilofsky, H. (1977) *J. Biol. Chem.* **252**, 6609–6616.
45. Padlan, E. A. (1990) *Proteins Struct. Funct. Genet.* **7**, 112–124.
46. Janin, J. & Chothia, C. (1990) *J. Biol. Chem.* **265**, 16027–16030.
47. Mian, I. S., Bradwell, A. R. & Olson, A. J. (1991) *J. Mol. Biol.* **217**, 133–151.
48. Lea, S. & Stuart, D. (1995) *FASEB J.* **9**, 87–93.
49. Grivel, J.-C. & Smith-Gill, S. J. (1995) in *Structure of Antigens*, ed. Van Regenmortel, M. H. (CRC, Boca Raton, FL), Vol. 3, p. 91.
50. Smith-Gill, S. J., Wilson, A. C., Potter, M., Prager, E. M., Feldmann, R. J. & Mainhart, C. R. (1982) *J. Immunol.* **128**, 314–322.
51. Cunningham, B. C. & Wells, J. A. (1993) *J. Mol. Biol.* **234**, 554–563.
52. Wells, J. A. (1996) *Proc. Natl. Acad. Sci. USA* **93**, 1–6.
53. Sharma, S., Georges, F., Klevit, R. E., Delbaere, L. T. J., Lee, J. S. & Waygood, E. B. (1991) *Proc. Natl. Acad. Sci. USA* **88**, 4877–4881.
54. Klevit, R. E. & Waygood, E. B. (1986) *Biochemistry* **25**, 7774–7781.
55. El-Kabbani, O. A., Waygood, E. B. & Delbaere, L. T. (1987) *J. Biol. Chem.* **262**, 12926–12929.
56. Paterson, Y., Englander, S. W. & Roder, H. (1990) *Science* **249**, 755–759.
57. Mylvaganam, S. E., Paterson, Y., Kaiser, K., Bowdish, K. & Getzoff, E. D. (1991) *J. Mol. Biol.* **221**, 455–462.
58. Davies, D. R. & Padlan, E. A. (1992) *Curr. Biol.* **2**, 254–256.
59. Stanfield, R. L., Takimoto-Kamimura, M., Rini, J. M., Profy, A. T. & Wilson, I. A. (1993) *Structure* **1**, 83–93.
60. Kurinov, I. V. & Harrison, R. W. (1995) *Acta Crystallogr. D* **51**, 98–109.
61. Harata, K. (1994) *Acta Crystallogr. D* **50**, 250–257.
62. Ramanadham, M., Sieker, L. C. & Jensen, L. H. (1990) *Acta Crystallogr. B* **46**, 63–69.
63. Clackson, T. & Wells, J. A. (1995) *Science* **267**, 383–386.
64. Chacko, S., Silverton, E., Kam-Morgan, L., Smith-Gill, S., Cohen, G. & Davies, D. (1995) *J. Mol. Biol.* **245**, 261–274.
65. Lavoie, T. B., Kam-Morgan, L. N. W., Mallet, C. P., Schilling, J. W., Prager, E. M., Wilson, A. C. & Smith-Gill, S. J. (1990) in *Use of X-ray Crystallography in the Design of Antiviral Agents*, eds. Laver, W. & Air, G. M. (Academic, San Diego), p. 213.
66. Tulip, W. R., Varghese, J. N., Webster, R. G., Laver, W. G. & Colman, P. M. (1992) *J. Mol. Biol.* **227**, 149–159.
67. Ysern, X., Fields, B. A., Bhat, T. N., Goldbaum, F. A., Dall'Acqua, W., Schwarz, F. P., Poljak, R. & Mariuzza, R. A. (1994) *J. Mol. Biol.* **238**, 496–500.
68. Jones, S. & Thornton, J. M. (1996) *Proc. Natl. Acad. Sci. USA* **93**, 13–20.
69. Cohen, G. H., Sheriff, S. & Davies, D. R. (1996) *Acta Crystallogr. D*, in press.